Matrix-product-state method with a dynamical local basis optimization for bosonic systems out of equilibrium

C. Brockt,[1,*] F. Dorfner,[2] L. Vidmar,[2] F. Heidrich-Meisner,[2] and E. Jeckelmann[1]

[1]*Institut für Theoretische Physik, Leibniz Universität Hannover, Appelstrasse 2, D-30167 Hannover, Germany*
[2]*Department of Physics and Arnold Sommerfeld Center for Theoretical Physics, Ludwig-Maximilians-Universität München, D-80333 München, Germany*

We present a method for simulating the time evolution of one-dimensional correlated electron-phonon systems which combines the time-evolving block decimation algorithm with a dynamical optimization of the local basis. This approach can reduce the computational cost by orders of magnitude when boson fluctuations are large. The method is demonstrated on the nonequilibrium Holstein polaron by comparison with exact simulations in a limited functional space and on the scattering of an electronic wave packet by local phonon modes. Our study of the scattering problem reveals a rich physics including transient self-trapping and dissipation.

Phonon degrees of freedom play an important role in the nonequilibrium properties of correlated materials. In particular, time-resolved spectroscopy [1,2], photoinduced phase transitions [3,4], and transport through low-dimensional or molecular junctions [5–7] call for theoretical investigations of the nonequilibrium dynamics of charge carriers coupled to lattice vibrations. Quantum lattice models such as the Holstein model [8] are often used to describe the low-energy properties of strongly correlated electron-phonon (EP) systems. Analytical studies of these systems out of equilibrium are very difficult and reliable results are scarce. Therefore, theorists often turn to numerical methods to investigate them [9–11]. However, accurate numerical simulations of correlated lattice systems are very challenging because of the rapid increase of the Hilbert space dimension with system size and phonon number fluctuations. Similarly, computing the nonequilibrium dynamics of correlated bosons is a significant challenge in a great variety of physical systems, such as nonlinear optical systems [12,13], quantum dissipative systems [14,15], and low-energy models of quantum chromodynamics [16].

In this Rapid Communication we present a method for simulating the time evolution of one-dimensional (1D) lattice models with strongly fluctuating bosonic degrees of freedom for long periods of time. It combines the time-evolving block decimation (TEBD) [17,18] with a local basis optimization (LBO) approach [19] to significantly reduce the computational cost. The key idea is to optimize the local bases for the bosonic degrees of freedom dynamically and adaptively. The accuracy of the method is first demonstrated by comparison with reliable results for a nonequilibrium polaron problem [20]. Then, its performance is illustrated with a study of wave packet scattering by a small EP-coupled structure.

In quantum lattice models phonon degrees of freedom are represented by bosonic sites. As the Hilbert space of a single bosonic site is already infinite, it must be truncated to a subspace of dimension M from the start in wave-function-based numerical approaches [9]. The most common choice is to use the lowest M eigenstates of a (well chosen) boson number operator $b^\dagger b$ defining a bare boson basis. Then, exact

diagonalization or exact time propagation can be easily performed, but the computational cost increases very rapidly with M and exponentially with the number of lattice sites. Matrix-product-state (MPS) algorithms, such as the density-matrix renormalization group (DMRG) [21–25] and TEBD, allow us to treat 1D systems at a lower computational cost and thus to investigate much larger systems. However, the computational effort still increases as M^3. Therefore, most applications have been restricted to problems with small phonon fluctuations ($M \lesssim 10$), in particular, for nonequilibrium problems [26].

Instead of a bare boson basis of dimension M, one can describe a quantum state $|\psi\rangle$ using an optimal local basis of dimension $M_O \leqslant M$, which is defined as the eigenbasis of the reduced density matrix of $|\psi\rangle$ for the bosonic site [19]. This approach is very efficient for ground-state calculations because a sufficient accuracy can be reached with a small optimal basis even when a very large bare basis would be required. As the optimal basis must be calculated self-consistently, the total computational cost still rises with M, but only linearly. Thus ground-state calculations can be carried out with exact diagonalization or MPS algorithms for systems with $M \geqslant 10^3$ using only moderate computer resources [9,19,27,28].

The LBO has yet to have been combined successfully with MPS methods to study EP systems out of equilibrium, but for a very recent study of the spin-boson model [29]. The key problem is that the local optimal basis depends on the represented quantum state $|\psi(t)\rangle$ and thus evolves with time. This is clearly seen in our recent study of the optimal boson basis for a nonequilibrium polaron problem (see Figs. 18–20 in Ref. [20]). Therefore, we have developed an algorithm which allows us to optimize the local basis dynamically for the evolving target state $|\psi(t)\rangle$.

We have implemented this approach within the TEBD algorithm [17,18], which is one of the simplest time-dependent MPS methods [30–32]. For a chain with L sites, the MPS representation of a quantum state $|\psi\rangle$ in an occupation number basis is

$$\psi(k_1, \ldots, k_L) = \Gamma^{1,k_1} \lambda^1 \Gamma^{2,k_2} \lambda^2 \cdots \lambda^{L-1} \Gamma^{L,k_L}, \quad (1)$$

where the indices k_j label the basis states of the d_j-dimensional Hilbert space representing the degrees of freedom on the lattice site $j \in \{1, \ldots, L\}$. (For a bosonic site, $d_j = M$.) The
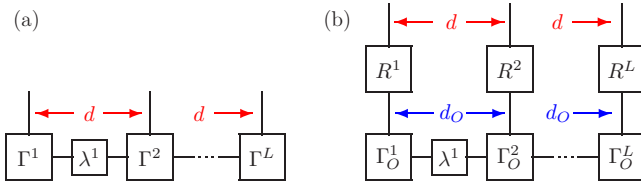
(a)

(b)

FIG. 1. (Color online) Graphical representation of the MPS (a) in the original TEBD algorithm and (b) in the TEBD-LBO algorithm.

entanglement between two parts of the lattice (e.g., the sites $\{1, \ldots, j\}$ and the sites $\{j+1, \ldots, L\}$) is encoded in the D_j-dimensional positive definite diagonal matrices λ^j. Hence the matrices Γ^{j,k_j} have dimensions $D_{j-1} \times D_j$ (with $D_0 = D_L = 1$). This MPS is represented graphically in Fig. 1(a). We call $D = \max\{D_1, \ldots, D_{L-1}\}$ the bond dimension of the MPS and $d = \max\{d_1, \ldots, d_L\}$ its local dimension.

Using orthogonality relations for the matrices Γ and λ, the matrix elements of the reduced density matrix ρ^j for the site j are given by

$$\rho^j_{k_j, k'_j} = \text{Tr}[(\Gamma^{j,k'_j})^\dagger (\lambda^{j-1})^2 \Gamma^{j,k_j} (\lambda^j)^2]. \tag{2}$$

The eigenbasis of this $d_j \times d_j$ matrix is called the optimal local basis. The unitary transformation from the optimal to the bare basis representation is denoted by R^j,

$$\Gamma^{j,k_j} = \sum_{s_j=1}^{d_O} R^j_{k_j, s_j} \Gamma^{j,s_j}_O. \tag{3}$$

This transformation is exact if $d_O = d_j$. The matrices λ^j are not affected by the basis change. The new MPS structure is illustrated in Fig. 1(b). This transformation of the matrices Γ in the TEBD algorithm is similar to the approach proposed for a variational MPS [28,33]. Each optimal basis state has a weight (eigenvalue) in the interval [0,1]. We can thus approximate the original state (1) using only the d_O ($\leqslant d$) eigenstates with the highest weights.

For a Hamiltonian which includes only on-site and nearest-neighbor interactions $H = \sum_j H_{j,j+1}$, the time evolution of the MPS (1) can be decomposed into successive local updates with a time step τ using a Trotter-Suzuki decomposition (TSD) of the time evolution operator $\tilde{\psi} = e^{-i\tau H_{j,j+1}} \psi$, where the local operator $H_{j,j+1}$ acts only on a single bond (i.e., sites j and $j+1$) [17,18]. Each local update is a unitary transformation which modifies the two matrices Γ and the one matrix λ associated with a bond. In practice, we use a second-order TSD resulting in an error $O(\tau^3)$ per time step or $O(\tau^2)$ for a finite period of time.

Here, we only explain how we perform the local update in our TEBD-LBO algorithm as our method is otherwise identical to the original TEBD [17,18]. We assume that we know the MPS (1) at a given time t in its truncated optimal local basis, i.e., we know the Γ_O, λ, and R matrices with $d_j \leqslant d_O \leqslant d$. A local update for a single bond consists of four steps. First, we build the rank-four tensor,

$$\phi^{k_j, k_{j+1}}_{\alpha_1, \alpha_2} = [\lambda^{j-1} \Gamma^{j,k_j} \lambda^j \Gamma^{j+1,k_{j+1}} \lambda^{j+1}]_{\alpha_1, \alpha_2}, \tag{4}$$

where the Γ matrices are given by (3) and the indices $\alpha_{1,2} = 1, \ldots, D$ number the matrix rows and columns. Then, in a

second step, we carry out the time evolution as done in the original TEBD algorithm,

$$\tilde{\phi}^{l_j, l_{j+1}}_{\alpha_1, \alpha_2} = \sum_{k_j, k_{j+1}} U^{l_j, l_{j+1}}_{k_j, k_{j+1}} \phi^{k_j, k_{j+1}}_{\alpha_1, \alpha_2}, \tag{5}$$

where U denotes the $d_j d_{j+1} \times d_j d_{j+1}$ matrix representation of the local time-evolution operator $e^{-i\tau H_{j,j+1}}$ in the bare basis. Generally, the computational cost for this step is $O(d^4 D^2)$, but it can be reduced to $O(d^2 D^2)$ using the sparseness of the matrix representation of (7) in a bare boson basis. In the third step, we compute the local reduced density matrix (2) from the tensor $\tilde{\phi}$ using the relation

$$\rho^j_{k_j, k'_j} = \sum_{k_{j+1}, \alpha_1, \alpha_2} \text{Tr}\big[\tilde{\phi}^{k_j, k_{j+1}}_{\alpha_1, \alpha_2} (\tilde{\phi}^{k'_j, k_{j+1}}_{\alpha_1, \alpha_2})^*\big] \tag{6}$$

and then diagonalize it. This yields the new optimal bases for the sites j and $j+1$, i.e., new transformations $\tilde{R}^j$ and $\tilde{R}^{j+1}$. We discard the optimal eigenstates with a negligible weight (e.g., lower than 10^{-13}) and thus obtain a new truncated optimal basis of dimension $\tilde{d}_O \leqslant d$. The tensor $\tilde{\phi}$ is then projected into the new optimal basis. Finally, in a fourth step, the new matrices $\tilde{\Gamma}^j_O$, $\tilde{\Gamma}^{j+1}_O$, and $\tilde{\lambda}^j$ are calculated from the projected tensor $\tilde{\phi}_O$ exactly as in the original TEBD algorithm. Hence we obtain the MPS representation of the state $\tilde{\psi}$ at time $t + \tau$ in its optimal local basis.

In summary, we repeatedly propagate the wave function (1) in a bare local basis to enlarge the effective Hilbert space and then project it onto a new effective Hilbert space using the LBO to control the dimension of the MPS. If $d_O \lesssim d$, the total computational effort scales as $d^3 D^3$, exactly as with a bare basis. If a small optimal basis is sufficient ($d_O \ll d$), however, our algorithm scales as the largest of $d_O^3 D^3$ (the computational cost of TEBD in the optimal basis) and $d^3 D^2$ (the computational cost for adapting the optimal basis), and thus it is significantly faster than a bare basis simulation. Contrary to the linear scaling of ground-state methods with d [9,19,28], however, the computational cost still increases as d^3, but the prefactor is reduced significantly, in particular, by a factor $\propto 1/D$. Therefore, the advantage of the TEBD-LBO will become more pronounced for problems with a large block entanglement, i.e., $D \gg 1$.

Next, we turn to two applications of our TEBD-LBO method to EP systems out of equilibrium. We consider an L_H-site Holstein chain [8] connected at each end to tight-binding leads with L_{TB} fermion sites. The Hamiltonian of the full system (with $L = L_H + 2L_{TB}$ sites) is

$$H = -t_0 \sum_{j=1}^{L-1} (c_j^\dagger c_{j+1} + c_{j+1}^\dagger c_j)$$

$$+ \sum_{j=L_{TB}+1}^{L_{TB}+L_H} [\omega_0 b_j^\dagger b_j - \gamma(b_j^\dagger + b_j) n_j], \tag{7}$$

where b_j and c_j annihilate a phonon (boson) and a (spinless) fermion on site j, respectively, and $n_j = c_j^\dagger c_j$. Thus $d = 2M$ in this model. The model parameters are the phonon frequency $\omega_0 > 0$, the EP coupling γ, and the hopping integral t_0. We work with $\hbar = 1$ and set the energy scale $t_0 = 1$, thus the time unit is $\hbar/t_0 = 1$.

Here, we restrict ourselves to the nonequilibrium dynamics of an electron coupled to phonons (i.e., the polaron dynamics), which has recently become a widely studied topic [20,34–45]. One-electron problems have MPS with low bond dimensions D, which can easily be simulated on a workstation when the effective local dimension is small (d or $d_O \lesssim 10$). Thus they provide us with a practical test field for our TEBD-LBO method. Typically, we used $D \leqslant 30$ or kept all block eigenstates with weight $>10^{-15}$ in combination with a time step τ as small as 10^{-3} to keep TEBD errors (induced by the TSD and the truncation of the bond dimensions) under control. The conservation of the electron number is used to decompose the matrices Γ, λ, ρ, and ϕ into block submatrices and thus speed up the calculations. Therefore, we also obtain different optimal boson states as a function of the electronic occupation of a site.

The initial wave function contains no phonon,

$$|\psi(t=0)\rangle = \sum_{j=1}^{L} f(j) c_j^\dagger |\emptyset\rangle, \qquad (8)$$

with the vacuum state $|\emptyset\rangle$. Thus it is only slightly entangled, as $D = d = 2$. Naturally, these dimensions can increase significantly when the wave function evolves with time [25]. Consequently, we always start our simulations with a small bare basis dimension d. After every time step τ, d is increased if the occupation of the highest phonon state exceeds some threshold (e.g., 10^{-7}).

First, we test our algorithm on the dynamics of a highly excited electron coupled to phonons [20]. In that case, no tight-binding lead is attached to the Holstein chain ($L = L_H$) and the electron is initially in a state $f(j) = \sqrt{2/(L+1)} \sin(Kj)$ with, e.g., $K = \pi L/(L+1)$. We have recently investigated this problem [20] using very accurate simulations within a limited functional space (LFS) [38,46], and we use these results to check the method presented here. As an illustration, Fig. 2 compares the time evolution of the phonon number $N_{ph} = \langle \sum_j b_j^\dagger b_j \rangle$ calculated using TEBD-LBO and LFS. In Fig. 2(a) we see that the agreement is very good, while in Fig. 2(b) we observe that relative deviations become overall smaller when the dimension d_O is increased and approach the values obtained using TEBD with a bare basis. Therefore, the global exponential increase of deviations with time is not due to the LBO but to intrinsic numerical errors of the TEBD and LFS methods. However, our tests also confirm that for this problem
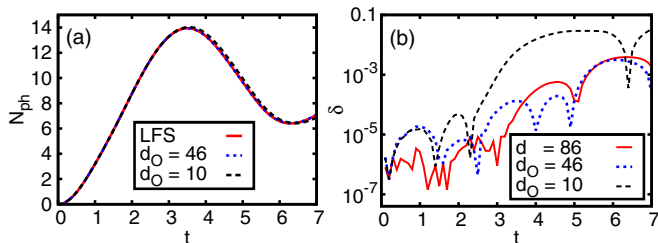

FIG. 2. (Color online) Comparison of LFS and TEBD-LBO for various d_O. (a) Time evolution of the phonon number calculated for $L = L_H = 6$, $\gamma = 2$, and $\omega_0 = 1$. (b) Relative deviations of the TEBD-LBO data from the LFS results. Deviations for TEBD with a bare basis of dimension $d = 86$ are also shown.

d_O must be a substantial fraction of the bare basis dimension d (e.g., $d_O \approx d/4$) to achieve a similar accuracy. Consequently, the dynamical LBO does not reduce the computational cost significantly in comparison to the bare basis approach for this type of problem. This is due to the relatively broad distribution of the local density-matrix eigenvalues that we found in our previous work [20].

Second, we apply our method to the scattering of an electronic wave packet by a small EP-coupled structure. In that case the tight-binding leads are much longer than the Holstein chain (we use L_{TB} up to 280 and $L_H \leqslant 6$ sites). The initial state is a Gaussian wave packet centered around a site j_0 in the left lead and with a positive velocity $v_0 \approx 2t_0 \sin(K)$,

$$f(j) = C \exp\left[-\frac{(j-j_0)^2}{4\sigma^2}\right] \exp[iKj], \qquad (9)$$

where C is a normalization constant, $L_{TB} - j_0 \gg \sigma \gg 1$, and $\pi > K > 0$. For the calculations presented here, we use $\sigma = 5$ and $K = \pi/2$. After a time $t \approx (L_{TB} - j_0)/v$, the wave packet reaches the Holstein chain where it becomes temporarily self-trapped, and finally it is partially transmitted and reflected [47].

For this problem we find that the dynamical LBO reduces the computational effort substantially when bosonic fluctuations are large. For cases which can be simulated with both a bare basis and an optimized one, we already observe speed-up factors larger than 10. For instance, for $\omega_0 = 0.6$ and $\gamma = 2$, calculations with a bare basis of dimension $d = 124$ ($M = 62$) take 14 times longer than with an optimized basis of dimension $d_O = 9$, but both approaches yield similar results with relative deviations smaller than 10^{-3}. For larger phonon fluctuations, we can only complete simulations using TEBD-LBO. For instance, in the strong-coupling adiabatic regime ($\omega_0 = 0.2$ and $\gamma = 2$), the required bare basis dimension is of the order of 10^3, but we can perform the TEBD-LBO simulation using only up to $d_O = 23$ optimal states. Therefore, the dynamical LBO allows us to study regimes that we could not treat with the standard TEBD algorithm on our workstation. (For comparison, dimensions $d = 30$ and $D = 5$ were reported in Ref. [29].)

The direct injection of an electronic wave packet into an EP-coupled chain was studied previously [34,37] but the scenario considered here has not yet been studied. Thus we briefly discuss two interesting phenomena that we have observed but postpone a more thorough discussion to a future work. The first phenomenon is the temporary self-trapping of the electron in the EP-coupled structure. In Fig. 3(a) we see that the electron reaches the EP-coupled structure at $t \approx 30$, but that a finite density remains in that region even for $t = 150$ [47]. At several times, fractions of the wave packet leave the Holstein chain and start to propagate in the leads. The probability of finding the electron in the Holstein chain $n_H = \sum_{j=L_{TB}+1}^{L_{TB}+L_H} \langle n_j \rangle$ is shown in Fig. 3(b). It increases rapidly when the wave packet reaches the left edge site of the Holstein chain at $t \approx 30$ and then decays exponentially fast for longer times. The decay rate is longer for longer chains. Therefore, (a fraction of) the electronic wave packet becomes temporarily self-trapped in the EP-coupled structure and is belatedly transmitted or reflected.

The second phenomenon is the dissipation of the electron energy due to inelastic scattering processes. Figure 4(a) shows
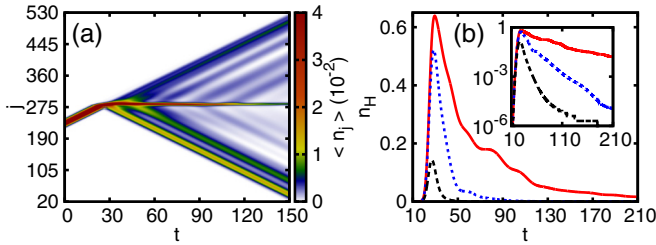
FIG. 3. (Color online) (a) Electronic density $\langle n_j \rangle$ as a function of site j and time t for $L_H = 6$, $\gamma = 1$, and $\omega_0 = 2.25$. The Holstein chain corresponds to sites $j = 280, \ldots, 285$. (b) Total electronic density n_H in a Holstein chain of length $L_H = 6$ (red solid line), 3 (blue dotted line), and 1 (black dashed line) as a function of time t. The inset shows the same data on a logarithmic scale.

FIG. 4. (Color online) (a) Electronic density $\langle n_j \rangle$ as a function of site j and time t for $L_H = 1$, $\gamma = 2.5$, and $\omega_0 = 1.65$. The position of the EP site is $j = 90$. (b) Phonon energy $E_{\mathrm{ph}} = \omega_0 N_{\mathrm{ph}}$ as a function of time for $L_H = 1$, $\omega_0 = 1.5$, and several values of γ.

that one pair of transmitted and reflected wave packets moves with the same absolute velocity $v_0 = 2$ as the incident wave packet while a second pair moves with a lower velocity $v_1 \approx 1.1$ [47]. This corresponds to an inelastic process where a phonon is excited by the presence of the electron in the EP-coupled structure and is then left behind when the electron propagates away from this structure. The final velocity $v_n = 2t_0 \sin(k_n)$ can be easily determined from the equality of the asymptotic total energy for $t \to \pm\infty$, $-2t_0 \cos(K) = n\omega_0 - 2t_0 \cos(k_n)$, where n is the number of excited phonons left behind. Similar patterns have been observed recently in a 1D photonic waveguide coupled to a two-level scatterer (see Fig. 3 in Ref. [48]). In Fig. 4(b) we see that the phonon energy $E_{\mathrm{ph}} = \omega_0 N_{\mathrm{ph}}$, which is zero initially, remains finite after the electron has left the EP-coupled structure (i.e., for $t \to \infty$). This confirms that an irreversible energy transfer occurs from the electron to the phonon degrees of freedom (dissipation).

In summary, we have developed a TEBD algorithm with a dynamical optimization of local boson bases that allows us
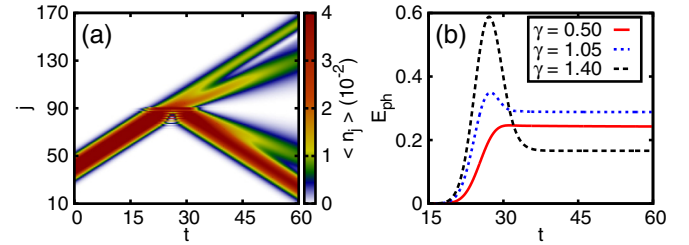
to simulate the nonequilibrium dynamics of electron-phonon systems more efficiently. This opens the way for numerous theoretical investigations of time-resolved spectral properties [1,2], photoinduced phase transitions [3,4], and transport in low dimensions [5–7]. The overall performance depends on the properties of the local density matrix out of equilibrium and thus on the specific problem investigated. The basic idea can easily be combined with other time-dependent MPS methods [30–32] or applied to other bosonic systems such as correlated photons [12,13], quantum baths [14,15], and scalar fields [16], as well as to other systems with large local Hilbert spaces such as high spin models [49,50].

[1] D. N. Basov, R. D. Averitt, D. van der Marel, M. Dressel, and K. Haule, Electrodynamics of correlated electron materials, Rev. Mod. Phys. **83**, 471 (2011).

[2] J. Orenstein, Ultrafast spectroscopy of quantum materials, Phys. Today **65**(9), 44 (2012).

[3] K. Nasu, Itinerant type many-body theories for photo-induced structural phase transitions, Rep. Prog. Phys. **67**, 1607 (2004).

[4] K. Yonemitsu and K. Nasu, Theory of photoinduced phase transitions in itinerant electron systems, Phys. Rep. **465**, 1 (2008).

[5] M. Galperin, M. A. Ratner, and A. Nitzan, Molecular transport junctions: vibrational effects, J. Phys.: Condens. Matter **19**, 103201 (2007).

[6] E. A. Osorio, T. Bjørnholm, J.-M. Lehn, M. Ruben, and H. S. J. van der Zant, Single-molecule transport in three-terminal devices, J. Phys.: Condens. Matter **20**, 374121 (2008).

[7] N. A. Zimbovskaya and M. R. Pederson, Electron transport through molecular junctions, Phys. Rep. **509**, 1 (2011).

[8] T. Holstein, Studies of polaron motion: Part I. The molecular-crystal model, Ann. Phys. **8**, 325 (1959).

[9] E. Jeckelmann and H. Fehske, Exact numerical methods for electron-phonon problems, Riv. Nuovo Cimento **30**, 259 (2007).

[10] F. F. Assaad and H. G. Evertz, World-line and Determinantal Quantum Monte Carlo Methods for Spins, Phonons and Electrons, in *Computational Many-Particle Physics*, edited by H. Fehske, R. Schneider, and A. Weiße, Lecture Notes in Physics Vol. 739 (Springer, Berlin, 2008), Chap. 10, pp. 277–356.

[11] M. Hohenadler and T. C. Lang, Autocorrelations in Quantum Monte Carlo Simulations of Electron-Phonon Models, in *Computational Many-Particle Physics* (Ref. [10]), Chap. 11, pp. 357–366.

[12] T. Grujic, S. R. Clark, D. Jaksch, and D. G. Angelakis, Non-equilibrium many-body effects in driven nonlinear resonator arrays, New J. Phys. **14**, 103025 (2012).

[13] I. Carusotto and C. Ciuti, Quantum fluids of light, Rev. Mod. Phys. **85**, 299 (2013).

[14] U. Weiss, *Quantum Dissipative Systems*, Series in Modern Condensed Matter Physics Vol. 13 (World Scientific, Singapore, 2008).

[15] Y. Yao, L. Duan, Z. Lü, C.-Q. Wu, and Y. Zhao, Dynamics of the sub-Ohmic spin-boson model: A comparison of three numerical approaches, Phys. Rev. E **88**, 023303 (2013).

[16] J. Berges, D. Gelfand, and D. Sexty, Amplified fermion production from overpopulated Bose fields, Phys. Rev. D **89**, 025001 (2014).

[17] G. Vidal, Efficient Classical Simulation of Slightly Entangled Quantum Computations, Phys. Rev. Lett. **91**, 147902 (2003).

[18] G. Vidal, Efficient Simulation of One-Dimensional Quantum Many-Body Systems, Phys. Rev. Lett. **93**, 040502 (2004).

[19] C. Zhang, E. Jeckelmann, and S. R. White, Density Matrix Approach to Local Hilbert Space Reduction, Phys. Rev. Lett. **80**, 2661 (1998).

[20] F. Dorfner, L. Vidmar, C. Brockt, E. Jeckelmann, and F. Heidrich-Meisner, Real-time decay of a highly excited charge carrier in the one-dimensional Holstein model, Phys. Rev. B **91**, 104302 (2015).

[21] S. R. White, Density Matrix Formulation for Quantum Renormalization Groups, Phys. Rev. Lett. **69**, 2863 (1992).

[22] S. R. White, Density-matrix algorithms for quantum renormalization groups, Phys. Rev. B **48**, 10345 (1993).

[23] U. Schollwöck, The density-matrix renormalization group, Rev. Mod. Phys. **77**, 259 (2005).

[24] E. Jeckelmann, Density-Matrix Renormalization Group Algorithms, in *Computational Many-Particle Physics* (Ref. [10]), Chap. 21, pp. 597–619.

[25] U. Schollwöck, The density-matrix renormalization group in the age of matrix product states, Ann. Phys. **326**, 96 (2011).

[26] H. Matsueda, S. Sota, T. Tohyama, and S. Maekawa, Relaxation dynamics of photocarriers in one-dimensional Mott insulators coupled to phonons, J. Phys. Soc. Jpn. **81**, 013701 (2012).

[27] W. Barford, R. J. Bursill, and M. Y. Lavrentiev, Breakdown of the adiabatic approximation in *trans*-polyacetylene, Phys. Rev. B **65**, 075107 (2002).

[28] C. Guo, A. Weichselbaum, J. von Delft, and M. Vojta, Critical and strong-coupling phases in one- and two-bath spin-boson models, Phys. Rev. Lett. **108**, 160401 (2012).

[29] F. A. Y. N. Schröder, A. W. Chin, and R. H. Friend, Simulating open quantum dynamics with time-dependent variational matrix product states: Towards microscopic correlation of environment dynamics and reduced system evolution, arXiv:1507.02202.

[30] S. R. White and A. E. Feiguin, Real-time evolution using the density matrix renormalization group, Phys. Rev. Lett. **93**, 076401 (2004).

[31] A. J. Daley, C. Kollath, U. Schollwöck, and G. Vidal, Time-dependent density-matrix renormalization-group using adaptive effective Hilbert spaces, J. Stat. Mech. (2004) P04005.

[32] P. Schmitteckert, Nonequilibrium electron transport using the density matrix renormalization group method, Phys. Rev. B **70**, 121302(R) (2004).

[33] B. Bruognolo, A. Weichselbaum, C. Guo, J. von Delft, I. Schneider, and M. Vojta, Two-bath spin-boson model: Phase diagram and critical properties, Phys. Rev. B **90**, 245130 (2014).

[34] L.-C. Ku and S. A. Trugman, Quantum dynamics of polaron formation, Phys. Rev. B **75**, 014307 (2007).

[35] D. M. Kennes and V. Meden, Relaxation dynamics of an exactly solvable electron-phonon model, Phys. Rev. B **82**, 085109 (2010).

[36] B. Luo, J. Ye, C. Guan, and Y. Zhao, Validity of time-dependent trial states for the Holstein polaron, Phys. Chem. Chem. Phys. **12**, 15073 (2010).

[37] H. Fehske, G. Wellein, and A. R. Bishop, Spatiotemporal evolution of polaronic states in finite quantum systems, Phys. Rev. B **83**, 075104 (2011).

[38] L. Vidmar, J. Bonča, M. Mierzejewski, P. Prelovšek, and S. A. Trugman, Nonequilibrium dynamics of the Holstein polaron driven by an external electric field, Phys. Rev. B **83**, 134301 (2011).

[39] D. Golež, J. Bonča, L. Vidmar, and S. A. Trugman, Relaxation Dynamics of the Holstein Polaron, Phys. Rev. Lett. **109**, 236402 (2012).

[40] G. Li, B. Movaghar, A. Nitzan, and M. A. Ratner, Polaron formation: Ehrenfest dynamics vs. exact results, J. Chem. Phys. **138**, 044112 (2013).

[41] A. Dey and S. Yarlagadda, Polaron dynamics and decoherence in an interacting two-spin system coupled to an optical-phonon environment, Phys. Rev. B **89**, 064311 (2014).

[42] P. Werner and M. Eckstein, Field-induced polaron formation in the Holstein-Hubbard model, Europhys. Lett. **109**, 37002 (2015).

[43] S. Sayyad and M. Eckstein, Coexistence of excited polarons and metastable delocalized states in photoinduced metals, Phys. Rev. B **91**, 104301 (2015).

[44] A. S. Mishchenko, N. Nagaosa, G. De Filippis, A. de Candia, and V. Cataudella, Mobility of Holstein Polaron at Finite Temperature: An Unbiased Approach, Phys. Rev. Lett. **114**, 146401 (2015).

[45] N. Zhou, Z. Huang, J. Zhu, V. Chernyak, and Y. Zhao, Polaron dynamics with a multitude of Davydov D2 trial states, J. Chem. Phys. **143**, 014113 (2015).

[46] J. Bonča, S. A. Trugman, and I. Batistić, Holstein polaron, Phys. Rev. B **60**, 1633 (1999).

[47] See Supplemental Material at http://link.aps.org/supplemental/10.1103/PhysRevB.92.241106 for movies of the time evolution of the electronic densities shown in Figs. 3(a) and 4(a).

[48] E. Sanchez-Burillo, D. Zueco, J. J. Garcia-Ripoll, and L. Martin-Moreno, Scattering in the Ultrastrong Regime: Nonlinear Optics With One Photon, Phys. Rev. Lett. **113**, 263604 (2014).

[49] S. Capponi, G. Roux, P. Lecheminant, P. Azaria, E. Boulat, and S. R. White, Molecular superfluid phase in systems of one-dimensional multicomponent fermionic cold atoms, Phys. Rev. A **77**, 013624 (2008).

[50] M. Führinger, S. Rachel, R. Thomale, M. Greiter, and P. Schmitteckert, DMRG studies of critical SU(N) spin chains, Ann. Phys. **17**, 922 (2008).